Classification and Lower Bounds for MEMS Arrays and Vibratory Parts Feeders: What Programmable Vector Fields Can (and Cannot) Do — Part I

Karl-Friedrich Böhringer, Bruce Randall Donald
Robotics & Vision Laboratory
Department of Computer Science
Noel C. MacDonald
School of Electrical Engineering and
The National Nanofabrication Facility
Cornell University, Ithaca, NY 14853

URL `http://www.cs.cornell.edu/Info/People/karl/MicroManipulation`

Abstract: *Programmable vector fields can be used to control a variety of flexible planar parts feeders. These devices can exploit exotic actuation technologies such as arrayed, massively-parallel microfabricated motion pixels or transversely vibrating (macroscopic) plates. These new automation designs promise great flexibility, speed, and dexterity—we believe they may be employed to orient, singulate, sort, feed, and assemble parts. However, since they have only recently been invented, programming and controlling them for manipulation tasks is challenging. By chaining together sequences of vector fields, the equilibrium states of a part in the field may be cascaded to obtain a desired final state. The resulting strategies require no sensing and enjoy efficient planning algorithms.*

This paper begins by describing our experimental devices. In particular, we describe our progress in building the M-Chip *(manipulation chip), a massively parallel array of programmable micromotion pixels. As proof of concept, we demonstrate a prototype* M-Chip *containing over 11,000 silicon actuators in one square inch. Both the* M-Chip*, as well as macroscopic devices such as transversely vibrating plates, may be programmed with vector fields, and their behavior predicted and controlled using our* equilibrium analysis*. We demonstrate lower bounds (i.e., impossibility results) on what the devices* cannot *do, and results on a classification of control strategies yielding design criteria by which well-behaved manipulation strategies may be developed. We provide sufficient conditions for programmable fields to induce well-behaved equilibria on every part placed on our devices. We define* composition operators *to build complex strategies from simple ones, and show the resulting fields are also well-behaved. We discuss whether fields outside this class can be useful and free of pathology.*

1 Introduction

Programmable vector fields can be used to control a variety of flexible planar parts feeders. These devices often exploit exotic actuation technologies such as arrayed, microfabricated motion pixels [5, 6] or transverse vibrating plates [1]. These new automation designs promise great flexibility, speed, and dexterity—we believe they may be employed to orient, singulate, sort, feed, and assemble parts (see for example Figures 1 or 7). However, since they have only recently been invented, programming and controlling them for manipulation tasks is challenging. Our research goal is to develop a science base for manipulation using programmable vector fields.

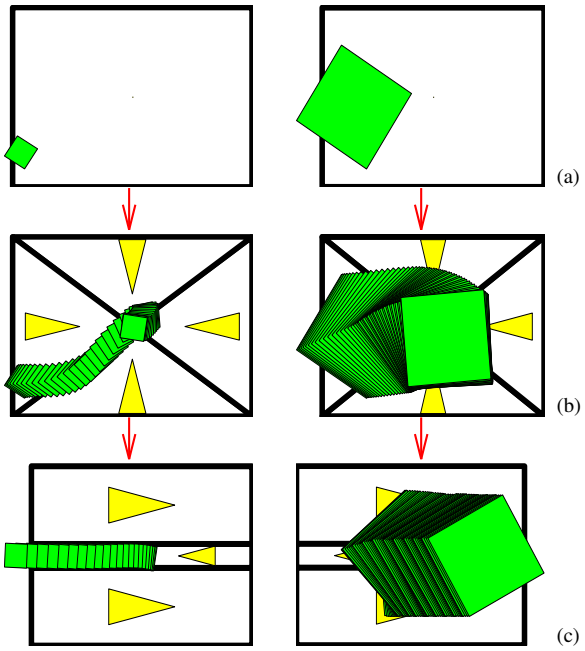

Figure 1: Sensorless sorting using force vector fields: Parts of various sizes are centered and subsequently separated depending on their size.

When a part is placed on our devices, the programmed vector field induces a force and moment upon it. Over time, the part may come to rest in a dynamic equilibrium state. In principle, we have tremendous flexibility in choosing the vector field, since using modern array technologies, the force field may be programmed pixel-wise. Hence, we have a lot of control over the resulting equilibrium states. By chaining together sequences of vector fields, the equilibria may be cascaded to obtain a desired final state—for example, this state may represent a unique orientation or pose of the part.

This paper (Part I) describes our experimental devices, a technique for analyzing them called *equilibrium analysis*, lower bounds (i.e., impossibility results) on what the devices *cannot* do, and results on a classification of control strategies yielding design criteria by which well-behaved manipulation strategies may be developed. Our companion paper (Part II [4]) describes new manipulation algorithms using the tools developed in Part I. In particular, we improve existing planning algorithms by a quadratic factor, show how to simultaneously orient and pose a part, and we relax earlier dynamic and mechanical assumptions to obtain more robust and flexible strategies.

What kinds of vector fields should we use for manipulation? In Part I, we ask *Which vector fields are suitable for manipulation strategies?* In particular, we ask whether the fields may be *classified.* That is: can we characterize all those vector fields in which every part has stable equilibria? While this question has been well-studied for a point mass in a field, the issue is more subtle when lifted to a body with finite area, due to the moment covector. To answer, we first demonstrate impossibility results, in the form of "lower bounds:" there exist perfectly plausible fields which induce *no* stable equilibrium in very simple parts.

Fortunately, there is also good news. We can provide sufficient conditions for fields to induce well-behaved equilibria when lifted, by exploiting the theory of potential fields. While potential fields have been widely used in robot control [15, 22, 21], micro-actuator arrays present us with

the ability to *explicitly* program the applied force *at every point* in a vector field. This alone makes our application of potential field theory to micro-devices unique and novel. Moreover, such fields can be composed using addition, sequential composition, "parallel" composition by superposition of controls, or by a new kind of "morphing" of control signals which we will define.

Previous results on array manipulation strategies may be formalized using *equilibrium analysis.* In [5] we proposed a family of control strategies called *squeeze patterns* and a planning algorithm for parts-orientation. This first result proved an $E = O(n^2)$ upper bound on the number of equilibria of a planar part with n vertices. This yields an $O(E^2) = O(n^4)$ planning algorithm to uniquely orient a part, under certain dynamic and mechanical assumptions. In Part I, we argue that the bound on equilibria appears tight. This results in a very high planning and execution complexity.

Using our equilibrium analysis, in Part I, we introduce *radial* fields, which satisfy our stability property. Radial fields can then be combined with squeeze fields. In Part II [4], we show this has several benefits. (1) The number of equilibria drops to $E = O(n)$. (2) The planning complexity drops to $O(E^2) = O(n^2)$. (3) Throughout the strategy execution, every part rotates about one fixed, unique point (after the first step). This means that (4) we can dispense with one critical assumption (called 2PHASE in [5]): we no longer need assume that the transitional and rotational motions induced by the array interact in a "quasi-static" and "sequential" manner.

We motivate our results by beginning Part I with a description of the experimental devices we are trying to program. In particular, we describe our progress in building the M-CHIP (manipulation chip), a massively parallel array of programmable micro-motion pixels. As proof of concept, we demonstrate a prototype M-CHIP containing over 11,000 silicon actuators in one square inch. Our strategies are also applicable to macroscopic parts-feeders. We describe a planar, vibratory orienting and manipulation device which also uses these novel strategies.

Both of these devices foreground several key practical issues. First, the radial strategies employed by our improved algorithms and analysis require significant mechanical and control complexity—even though they require no sensing. While we believe such mechanisms are feasible to build using the silicon MEMS (microelectromechanical systems) technologies we advocate, it is undeniable that no such device exists yet. (The M-CHIPS will have pixel-wise programmability, but the first generation will probably not have sufficient resolution to implement highly accurate radial strategies). For this reason, in Part II [4] we introduce and analyze strategies composed of field sequences that we know are implementable using current (microscopic or macroscopic) technology. Each strategy is a sequence of pairs of squeezes satisfying certain "orthogonality" properties. Under these assumptions, we can ensure (a) equilibrium stability, (b) relaxed mechanical and dynamical assumptions (the same as (4), above) and (c) complexity and completeness guarantees. The framework is quite general, and applies to any set of primitive operations satisfying certain "finite equilibrium" properties (which we define)—hence it has broad applicability to a wide range of devices. In particular, we view the restricted class of fields as a *vocabulary* and their rules of composition as a *grammar*, resulting in a "language" of manipulation strategies. Under our grammar, the resulting strategies are guaranteed to be well-behaved.

Finally, both our radial strategies and our *finite manipulation grammar* have the following advantage over previous manipulation algorithms for programmable vector fields: previous algorithms such as [5] guarantee to uniquely orient a part, but the transitional position of the part is unknown at the strategy's termination. Both of our new algorithms guarantee to position the part uniquely in translation *as well as* orientation space.

However, the complexity and completeness guarantees we obtain for manipulation grammars are considerably weaker than for the ideal radial strategies. For radial strategies, we show that *any* connected, planar part with finite area contact can be oriented within the complexity bounds

above. Under the simplified "manipulation grammar," our planner is guaranteed to find a strategy if one exists (If one does not exist, the planner will signal this). However, it is not known whether there exists a strategy for every part. Moreover, the planning algorithm is exponential instead of merely quadratic.

This result illustrates a tradeoff between mechanical complexity (the dexterity and controllability of field elements) and planning complexity (the computational difficulty of synthesizing a strategy). If one is willing to build a device capable of radial fields, then one reaps great benefits in planning and execution speed. On the other hand, we can still plan for simpler devices, but the plan synthesis is more expensive, and we lose some completeness properties.

Finally, the desire to implement complicated fields raises the question of control uncertainty. We close Part II [4] by describing how families of potential functions can be used to represent control uncertainty, and analyzed for their impact on equilibria.

2 Experimental Apparatus: Parts Feeders

It is often extremely costly to maintain part order throughout the manufacture cycle. Instead of keeping parts for example in pallets, they are often delivered in bags or boxes, from where they must be picked out and sorted. A parts feeder is a machine that orients such parts before they are fed to an assembly station. Currently, the design of parts feeders is a black art that is responsible for up to 30% of the cost and 50% of workcell failures [7, for example]. Thus although part feeding accounts for a large portion of assembly cost, there is not much scientific basis for automating the process.

The most common type of parts feeder is the *vibratory bowl feeder*, where parts in a bowl are vibrated with a rotary motion so that they climb a helical track. As they climb, a sequence of baffles and cutouts in the track create a mechanical "filter" that causes parts in all but one orientation to fall back into the bowl for another attempt at running the gauntlet [7]. Sony's APOS parts feeder [13] uses an array of nests (silhouette traps) cut into a vibrating plate. The nests and the vibratory motion are designed so that the part will remain in the nest only in a particular orientation. By tilting the plate and letting parts flow across it, the nests eventually fill up with parts in the desired orientation. Although the vibratory motion is under software control, specialized mechanical nests must be designed for each part [19].

The reason for the success of vibratory bowl feeders and the Sony APOS system is the underlying principle of *sensorless manipulation* [11] that allows parts positioning and orienting without sensor feedback. This principle is even more important at small scales, because sensor data will be less accurate and more difficult to obtain. The APOS system or bowl feeders are unlikely to work in the micro domain: instead novel device designs for micro-manipulation tasks are required. The theory of sensorless manipulation is the science base for developing and controlling such devices.

Reducing the amount of required sensing is an example of *minimalism* [2, 9], which pursues the following agenda: For a given robot task, find the minimal configuration of resources required to solve the task. Minimalism is interesting because doing task A without resource B proves that B is somehow inessential to the information structure of the task. In robotics, minimalism has become increasingly influential. Marc Raibert [20] showed that walking and running machines could be built without static stability. Erdmann and Mason [11] showed how to do dexterous manipulation without sensing. McGeer [17] built a biped, kneed walker without sensors, computers, or actuators. Canny and Goldberg [9] investigated robot systems with minimal intricacy. Rod Brooks [8] has developed online algorithms that rely less extensively on planning and world models. Donald et al. [10, 2] have built teams of mobile robots that cooperate in manipulation without explicit

communication. We use these results for our experiments in micro-manipulation, and we examine how they relate to our theoretical proofs of minimalist systems.

2.1 Microfabricated Actuator Arrays

A wide variety of micromechanical structures (devices typically in the μm range) has been built recently by using processing techniques known from VLSI industry. However, the fabrication, control, and programming of micro-devices that can interact and actively change their environment remains challenging. Problems arise from (1) unknown material properties and the lack of adequate models for mechanisms at very small scales, (2) the limited range of motion and force that can be generated with microactuators, (3) the lack of sufficient sensor information with regard to manipulation tasks, and (4) design limitations and geometric tolerances due to the fabrication process.

MEMS manipulator arrays have been proposed by several MEMS researchers, among other Fujita et al. [12], Will et al. [16], or Jacobson et al. [14]. For an overview see [6, 5] or [16]. Our arrays are fabricated using a SCREAM (Single-Crystal Reactive Etching and Metallization) process developed in the Cornell National Nanofabrication Facility [24, 23]. The SCREAM process is low-temperature, and does not interfere with traditional VLSI. Hence it opens the door to building monolithic microelectromechanical systems with integrated microactuators and control circuitry on the same wafer.

Our design is based on microfabricated torsional resonators [18]. Each unit device consists of a rectangular grid etched out of single-crystal silicon suspended by two rods that act as torsional springs (Figure 3). The grid is about 200 μm long and extends 120 μm on each side of the rod. The rods are 150 μm long. The current asymmetric design has 5 μm high protruding tips on one side of the grid that make contact with an object lying on top of the actuator (Figure 4). The other side of the grid consists of a denser grid above an aluminum electrode. If a voltage is applied between grid and electrode, the half of the grid above the electrode is pulled downward by the resulting electrostatic force. Simultaneously the other side of the grid (with the tips) is deflected out of the plane by several μm. Hence an object can be lifted and pushed sideways by the actuator.

Each actuator can generate motion in one specific direction if it is activated, otherwise it acts as a passive frictional contact. Figure 2 shows a small section of such a unidirectional actuator array, which consists of more than 11,000 individual actuators. The combination and selective activation of several actuators with different motion bias allows us to generate various motions in discrete directions, spanning the plane (Figure 5).

The fabrication process and mechanism analysis are described in more detail in the Appendix and in [6].

2.2 Macroscopic Vibratory Parts Feeder

Böhringer et al. [1] have presented a device that uses the force field created by transverse vibrations of a plate to position and align parts. The device consists of an aluminum plate that is attached to a commercially available electrodynamic vibration generator,[1] with a linear travel of 0.02 m, and capable of producing a force of up to 500 N (Figure 6). The input signal, specifying the waveform corresponding to the desired oscillations, is fed to a single coil armature, which moves in a constant field produced by a ceramic permanent magnet in a center gap configuration.

For low amplitudes and frequencies, the plate moves longitudinally with no perceptible transverse vibrations. However, as the frequency of oscillations is increased, transverse vibrations of the

[1] Model VT-100G, Vibration Test Systems, Akron, OH, USA.

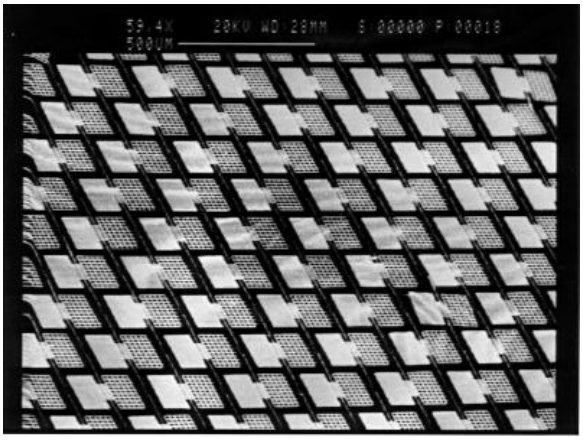

Figure 2: A prototype M-Chip fabricated in 1995. A large unidirectional actuator array (scanning electron microscopy). Each actuator is $180 \times 240\,\mu m^2$ in size. Detail from a 1 in^2 array with more than 11,000 actuators. For more pictures on device design and fabrication see URL `http://www.cs.cornell.edu/Info/People/karl/MicroActuators`.

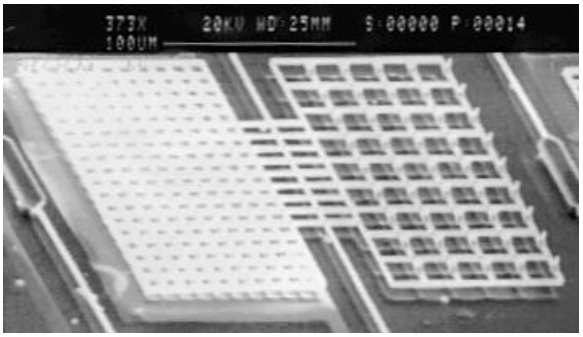

Figure 3: Released asymmetric actuator for the M-Chip (scanning electron microscopy). Left: Dense grid (10 μm spacing) with aluminum electrode underneath. Right: Grid with 5 μm high poles.

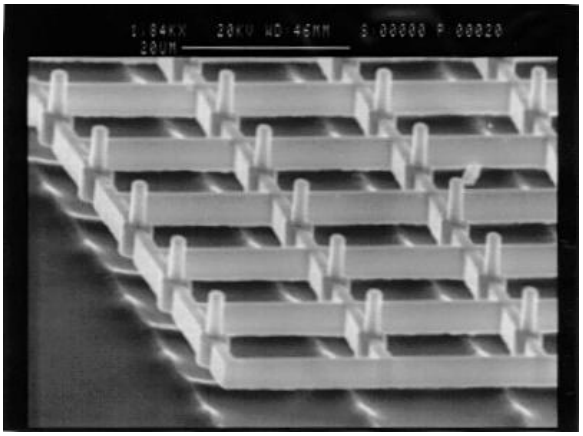

Figure 4: Released M-Chip actuators consisting of single-crystal silicon with 5 μm high tips.

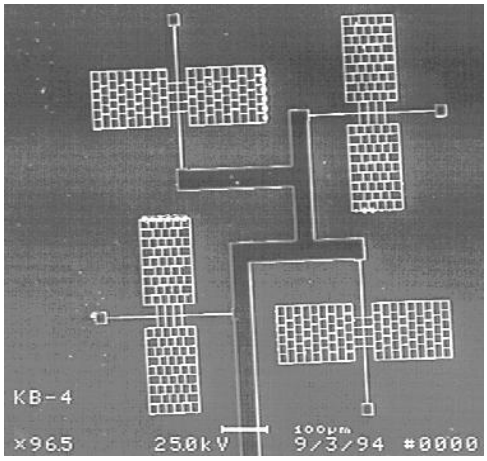

Figure 5: Released M-CHIP prototype motion pixel consisting of actuators oriented in four different directions.

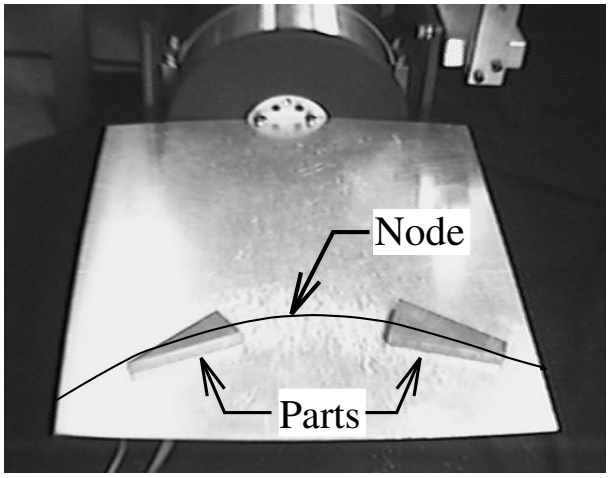

Figure 6: Vibratory parts feeder: the aluminum plate exhibits a vibratory minimum. Parts reach equilibrium along this node line. See also URL `http://www.cs.cornell.edu/Info/People/karl/VibratoryAlign`. Reproduced with permission from [1].

plate become more pronounced. The resulting motion is similar to the forced transverse vibration of a rectangular plate, clamped on one edge and free along the other three sides.

Figure 6 shows two planar shapes, a triangle and a trapezoid, after they have reached their stable position and orientation. To better illustrate the orienting effect, the curve showing the node has been drawn by hand. *Nota bene*: This device can only use the finite manipulation grammar since it can only generate a constrained set of vibratory patterns, and cannot implement radial strategies.

3 Equilibrium Analysis For Programmable Vector Fields

In [5] we proposed a family of control strategies called *squeeze fields* and a planning algorithm for parts-orientation.

Definition 1 [5] *Assume l is a straight line. A* squeeze field *F is a two-dimensional force field defined as follows: (1) If $z \in \mathbb{R}^2$ lies on l then $F(z) = 0$. (2) If z does not lie on l then $F(z)$ is the unit vector normal to l and pointing towards l.*

We refer to the line l as the squeeze line, because l lies in the center of the squeeze pattern. See Figure 7 for examples of squeeze fields. To model our actuator arrays and vibratory devices, we make the following assumptions:
DENSITY: The generated forces can be described by a vector field, i.e. the individual microactuators are dense compared to the size of the moving part.
2PHASE: The motion of a part has two phases: (1) Pure translation towards l until the part is in force equilibrium. (2) Motion in force equilibrium until moment equilibrium is reached, too.

Under these assumptions we showed in [5] that any connected polygonal part, when put in a squeeze field, reaches one of a *finite* number of possible equilibrium orientations. This can be used to generate manipulation plans that uniquely orient a given part (for example the two-step plan in Figure 7). Let us summarize these results as shown in [5]:

Theorem 2 [5] *For a simple polygonal part P and an actuator array $\mathcal{A}$ there exists an alignment strategy $\mathcal{S} = (l_1, \ldots, l_k)$ that uniquely aligns P up to symmetries.*

Corollary 3 [5] *If P is a n-gon, the algorithm runs in time $O(n^4)$ and produces a strategy $\mathcal{S} = (l_1, \ldots, l_k)$ of length $k = O(n^2)$. If P is convex the running time is $O(n^2)$ and $k = O(n)$.*

4 Lower bounds: What Programmable Vector Fields Cannot Do

We now present "lower bounds" — constituting vector fields and parts with pathological behavior, making them unusable for manipulation. These counterexamples show that we must be careful in choosing programmable vector fields, and that, *a priori*, it is not obvious when a field is well-behaved.

In Section 3 we saw that in a vector field with a simple squeeze pattern (see again Figure 7), polygonal parts reach certain equilibrium positions. This raises the question of a *general classification of all those vector fields in which every part has stable equilibria.* There exist vector fields that do not have this property even though they are very similar to a simple squeeze.

Proposition 4 *A skewed vector field induces* no *stable equilibrium on a disk-shaped part.*

Proof: Consider Figure 8: Only when the center of the disk coincides with the center of the squeeze pattern do the translational forces acting on the disk balance. But it will still experience a positive moment that will cause rotation. □

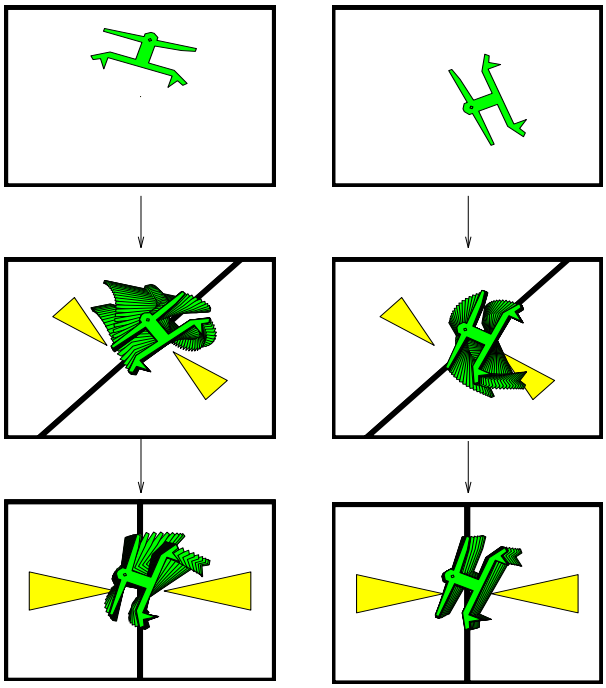

Figure 7: Sensorless parts alignment using force vector fields: Parts reach unique poses after two subsequent squeezes. See URL `http://www.cs.cornell.edu/Info/People/karl/MicroManipulation` for an animated simulation.

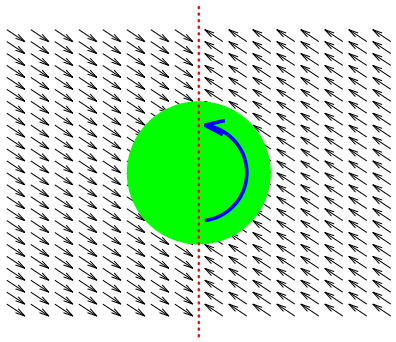

Figure 8: Unstable part in skewed squeeze field. The disk with center on the squeeze line will keep rotating. Moreover, it has *no* stable equilibrium in this field.

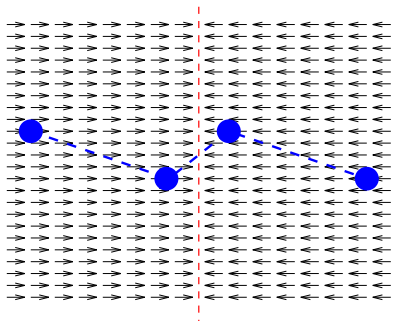

Figure 9: S-shaped part with four rigidly connected "feet" in unstable equilibrium (forces and moments balance). There exists *no* stable equilibrium position for this part in a vector field with a simple squeeze pattern.

Similarly we would like to identify the *class of all those parts that always reach stable equilibria* in particular vector fields. From Section 3 we know that connected polygons in simple squeeze fields have this property. This theorem relies on finite area contacts: it does not hold for point contacts. As a counterexample consider the part in Figure 9.

Proposition 5 *There exist parts that do not have stable equilibria in a simple squeeze field.*

Proof: The S-shaped part in Figure 9 has four rigidly connected "feet" with small contact surfaces. As the area of each of these four feet approaches zero, the part has *no* stable equilibrium in a simple squeeze field. There is only one orientation for the part in which both force and moment balances out, and this orientation is unstable. □

Finally, the *number of stable equilibria of a given part* influences both the planning complexity and the plan length of an alignment strategy. It also effects the resolution of the vector field that is necessary to perform a strategy accurately. Even though all parts we have considered, in practice, exhibit only one or two equilibria, there exist no tight bounds on the maximum number of equilibria.

Proposition 6

A. Regular polygons with n vertices have $\Omega(n)$ stable equilibria in a squeeze field.

B. All polygons have $O(n^2)$ stable equilibria in a squeeze field.

The $O(n^2)$ upper bound comes from the fact that there exist simple polygons with n vertices that can be bisected by a straight line in up to $O(n^2)$ topologically different ways [3]. This suggests that there could be parts that have $\Omega(n^2)$ equilibria in a squeeze field, which would imply alignment plans of length $\Omega(n^2)$ and planning complexity $\Omega(n^4)$.

While the counterexample in Figure 9 may be plausibly avoided by prohibiting parts with "point contacts," the other examples (Figure 8 and Proposition 6(B)) are more problematic. In Section 5, we show how to choose programmable vector fields that exclude these pathological behaviors, by using the theory of potential fields to describe a class of force vector fields for which *all* polygonal parts have stable equilibria.

We believe that fields without potential will often induce pathological behavior in many parts. However, there are some cases where non-potential fields may be useful. For example, see Figure 1c, which is *not* a potential field. Such fields may be employed to *separate* but not to stabilize, pose, or orient parts. This strong statement devolves to our proof that fields like Figure 8 do not have well-behaved equilibria. Hence, they should only be employed when we want to induce an unstable system that will cast parts away from equilibrium, e.g. in order to sort or separate them.

Similarly, we believe parts with point contact (not having finite area contact) will behave badly in *all* vector fields. Fields without potential admit paths along which a particle (point mass) will gain energy. Since mechanical parts are rigid aggregations of particles, this may induce unstable behavior in larger bodies. Similarly, point contact permits rapid, discontinuous changes in force and moment. Hence, bodies with point contact will tend to exhibit instabilities. Finally, we believe that as the area contact—the size of the "feet" of a part—approaches zero, the part may become unstable. This represents a design constraint on parts which are to be manipulated using programmable planar parts feeders.

The lower bounds we demonstrate are indications of the pathologies that can arise when fields without potential or parts with point contact are permitted. Each of our examples (Figures 8 and 9) is "generic" in that it can be generalized to a very large class of similar examples. However, these lower bounds are just a first step, and one wishes for examples that delineate the capabilities of programmable vector fields for planar parts manipulation even more precisely.

To summarize: We can show that the separating field shown in Figure 1c is not a potential field, and that there exist parts that will spin forever, without equilibrium, in this field (this follows by generalizing the construction in Figure 8). However, for *specific parts*, such as those shown in Figure 1, this field is useful if we can pose the parts appropriately first (e.g.. using the potential field shown in Figure 1b).

Finally, we may "surround" non-potential fields with potential fields to obtain reasonable behavior in some cases. For example, if field 1c is surrounded by a larger potential field, then after separation, parts can reach a stable equilibrium.

5 Completeness: Classification Using Potential Fields

In this section we give a family of vector fields that have proven useful for manipulation tasks. These fields belong to a specific class of vector fields: the class of fields that have a potential.

We are interested in a *general classification of all those vector fields in which every part has stable equilibria.* As motivation, recall that a skewed vector field, even though very similar to a regular squeeze pattern (see again Figure 7), induces *no* stable equilibrium in a disk-shaped part (Figure 8).

Consider the class of vector fields that have a *potential*, i.e. fields F in which the work is independent of the path, or equivalently, the work on any closed path is zero, $\oint F = 0$. In a

potential field each point (x, y) is assigned a value $U(x, y)$ that can be interpreted as its potential energy. When U is smooth, then the vector field F associated with U is the gradient $-\nabla U$. In general, $U(x, y)$ is given by the integral $\int_\alpha F$, where α is an arbitrary path from a fixed reference point (x_0, y_0) to (x, y).

An ideal point object is in stable equilibrium iff it is at a local minimum of U. For a part P of arbitrary shape we define the *lifted potential* $U_P : \mathcal{C} \to \mathbb{R}$, where $\mathcal{C} = \mathbb{R}^2 \times S^1$ is the configuration space of U_P, and U_P is defined as the area integral of the potential U over P in configuration (x, y, θ). Again, $U_P(x, y, \theta)$ can be interpreted as the potential energy of part P in configuration (x, y, θ).

One can show that the category of potential fields is closed under the operation of lifting. Therefore we obtain a lifted potential field U_P whose local minima are the stable equilibrium configurations in $\mathcal{C}$ for part P. Furthermore, potential fields are closed under addition. We can thus create and analyze more complex fields by looking at their components. In general, the theory of potential fields allows us to classify manipulation strategies with vector fields, offering new insights into equilibrium analysis and providing the means to determine strategies with stable equilibria. For example, it allows us to show that equilibrium in a simple squeeze field is equivalent to the stability of a homogeneous boat floating in water.

Radial fields. A *radial field* is a vector field whose forces are directed towards a specific center point. As a specific example, consider the *unit radial field* R which is defined (in polar coordinates) by $R(r, \theta) = r/||r||$ for $r \neq 0$, and $R(0, \theta) = 0$. Note that R has a discontinuity at the origin. A smooth radial field can be defined for example by $R'(r, \theta) = -r^2$.

Morphing and combining vector fields. Our strategies from Section [5] (see Section 3) have *switch points* in time where the vector field changes discontinuously (Figure 7). This is because we have shown that after one squeeze, for every part, the equilibrium is in a finite set of possible configurations, but in general non-unique. Hence subsequent squeezes are needed to disambiguate its pose. Therefore this switch is necessary for strategies with squeeze patterns.

One may ask whether for another class of potential field strategies, *unique* equilibria may be obtained without discrete switching. We believe that *continuously varying* vector fields of the form $(1-t)F + t\,G$, where $t \in [0, 1]$ represents time, and F and G are squeezes, may lead to vector fields that have this property (see Part II [4] for progress in this direction). Here "+" denotes point-wise addition of vector fields, and we will write "$F \rightsquigarrow G$" for the resulting continuously varying field. By restricting F and G to be fields with potential, we guarantee that $F+G$ and $F \rightsquigarrow G$ are well-behaved strategies. These form the basis of our new algorithms in Part II [4].

Theorem 7 *Every potential field with at least one local minimum induces stable equilibria for all planar parts with finite contact area.*

Because of Theorem 7, the use of potential fields is invaluable for the analysis of effective and efficient manipulation strategies, as discussed in Part II [4]. In particular, it is useful for proving the completeness of a manipulation planner.

Acknowledgments

We thank Dan Halperin for useful discussions and valuable comments, and Jean-Claude Latombe for his hospitality during our stay at the Stanford Robotics Laboratory.

Support is provided in part by the NSF under grants No. IRI-8802390, IRI-9000532, IRI-9201699, and by a Presidential Young Investigator award to Bruce Donald, in part by NSF/ARPA Special Grant for Experimental Research No. IRI-9403903, and in part by the AFOfSR, the Mathematical Sciences Institute, Intel Corporation, and AT&T Bell laboratories. This work was supported by ARPA under contract DABT 63-69-C-0019. The device fabrication was performed at the National Nanofabrication Facility (CNF), which is supported by the NSF grant ECS-8619049, Cornell University, and Industrial Affiliates.

Appendix — Single-Crystal Silicon Actuator Arrays for Micro Manipulation Tasks

Summary: Arrays of electrostatic actuators have been fabricated using a modified, multi-layer SCREAM (single-crystal reactive etching and metallization) process. These MEMS arrays are used to generate a force field for the manipulation of flat objects. First experiments with pieces of glass show that the actuator array is strong enough to move macroscopic objects. The size of a monolithic array reaches up to one square inch, with more than 11,000 individual single-crystal silicon torsional actuators on one chip. Larger arrays in currently being built.

SCS Torsional Actuators

A torsional actuator consists of a rectangular grid etched out of single-crystal silicon suspended by two rods that act as torsional springs (Figure 3). The grid is about 200 μm long and extends 120 μm on each side of the rod. The rods are 150 μm long. The current asymmetric design has 5 μm high protruding tips (Figure 4) on one side of the grid that make contact with an object lying on top of the actuator. The other side of the grid consists of a denser grid above an aluminum electrode. If a voltage is applied between grid and electrode, the half of the grid above the electrode is pulled downward by the resulting electrostatic force. Simultaneously the other side of the grid (with the tips) is deflected out of the plane by several μm. Hence an object can be lifted and pushed sideways by the actuator.

Because of its low inertia (resonance in the high kHz range) the device can be driven in a wide frequency range from DC to several 100 kHz AC. Due to the asymmetry in the actuator design, each actuator can generate motion in one specific direction if it is activated; otherwise it acts as a passive frictional contact. Figure 2 shows a small portion of such a unidirectional actuator array, which consists of more than 11,000 individual actuators that cover most of the substrate surface (Figure 2). The layout of the array can be changed such that the actuators point in various orientations. The combination and selective activation of several actuators in different orientations allows us to generate various motions in discrete directions, spanning the plane.

Fabrication Process

The actuator tips are patterned in a photolithography step on a layer of mask SiO_2. After pattern transfer, a high aspect ratio RIE chlorine etch is performed to obtain the tips. Then we perform a standard SCREAM process: A second photolithography step and similar RIE etches create the actuator grids. We use an isotropic SF_6 etch to release the actuators.

After the release, a thin film of dielectric SiO_2 is deposited, and a layer of aluminum is sputtered onto the substrate, making sure that the surface under the actuator grid is fully covered with aluminum. The electrodes are patterned in a third photolithography step.

The actuators consist of beams that are close to $1\,\mu m$ wide and $5\,\mu m$ high, with $\approx 5\,\mu m$ clearance underneath. Our current actuator designs have grids of $100 - 200\,\mu m$ side length. The fabrication can be done in one to two weeks in the National Nanofabrication Facility (CNF) at Cornell University.

Experiments

First manipulation experiments have been performed on a prototype array with more than 11,000 individual actuators, each of them weighing about $5 \cdot 10^{-5} \mu g$. The manipulation experiments were performed with small

glass pieces of a few mm^2 size and about $1\,\mu g$ weight. The experiments showed that our devices are strong enough to lift or move objects heavier than paper. Based on these experiments, an improved prototype actuator array with higher tips and more out-of-plane motion is currently being built.

The current devices exhibit a rather low yield of about 30 % working devices in one array. This mainly due to the experimental nature of the first fabrication process. We expect much better yield in the next generation.

Conclusions and Future Work

We present a process for the fabrication of single-crystal silicon electrostatic actuator arrays that are strong enough to perform useful manipulation tasks. This process is low-temperature and compatible with traditional VLSI. Process extensions to integrate electronic circuitry *in* the devices are under development. This opens the door for a wide range of manipulator control strategies.

In earlier work we have presented several strategies for sorting, positioning, and orienting parts (Figures 1 and 7). These strategies were interesting because they require no sensor input. Instead, we predict the stable equilibrium positions in which moving parts will end up by analyzing the force field that the actuators generate. These strategies have been proven useful in theoretical analyses and simulations by various researchers. We will test these strategies with the next generation of our actuator array.

References

[1] K.-F. Böhringer, V. Bhatt, and K. Y. Goldberg. Sensorless manipulation using transverse vibrations of a plate. In *Proc. IEEE Int. Conf. on Robotics and Automation (ICRA)*, Nagoya, Japan, May 1995. URL http://www.cs.cornell.edu/Info/People/karl/VibratoryAlign.

[2] K.-F. Böhringer, R. G. Brown, B. R. Donald, J. S. Jennings, and D. Rus. Distributed robotic manipulation: Experiments in minimalism. In *Fourth International Symposium on Experimental Robotics (ISER)*, Stanford, California, June 1995. URL ftp://ftp.cs.cornell.edu/pub/brd/brd.html.

[3] K.-F. Böhringer, B. R. Donald, and D. Halperin, 1995. Personal communication / in preparation.

[4] K.-F. Böhringer, B. R. Donald, and N. C. MacDonald. What programmable vector fields can (and cannot) do: Part II — new and improved manipulation algorithms for MEMS arrays and vibratory parts feeders. Technical report, Cornell University, Robotics and Vision Laboratory, Ithaca, NY, Oct. 1995. URL http://www.cs.cornell.edu/Info/People/karl/MicroManipulation.

[5] K.-F. Böhringer, B. R. Donald, R. Mihailovich, and N. C. MacDonald. Sensorless manipulation using massively parallel microfabricated actuator arrays. In *Proc. IEEE Int. Conf. on Robotics and Automation (ICRA)*, pages 826–833, San Diego, CA, May 1994. URL http://www.cs.cornell.edu /Info/People/karl/MicroManipulation.

[6] K.-F. Böhringer, B. R. Donald, R. Mihailovich, and N. C. MacDonald. A theory of manipulation and control for microfabricated actuator arrays. In *Proc. IEEE Workshop on Micro Electro Mechanical Systems (MEMS)*, pages 102–107, Oiso, Japan, Jan. 1994. URL http://www.cs.cornell.edu /Info/People/karl/MicroActuators.

[7] G. Boothroyd, C. Poli, and L. E. Murch. *Automatic Assembly.* Marcel Dekker, Inc., 1982.

[8] R. Brooks. A layered intelligent control system for a mobile robot. *IEEE Journal of Robotics and Automation*, RA(2), 1986.

[9] J. Canny and K. Goldberg. "RISC" for industrial robotics: Recent results and open problems. In *Proc. IEEE Int. Conf. on Robotics and Automation (ICRA).* IEEE, May 1994.

[10] B. R. Donald, J. Jennings, and D. Rus. Information invariants for distributed manipulation. In K. Goldberg, D. Halperin, J.-C. Latombe, and R. Wilson, editors, *Algorithmic Foundations of Robotics*, pages 431–459, Wellesley, MA, 1995. K. Peters.

[11] M. A. Erdmann and M. T. Mason. An exploration of sensorless manipulation. *IEEE Journal of Robotics and Automation*, 4(4), Aug. 1988.

[12] H. Fujita. Group work of microactuators. In *International Advanced Robot Program Workshop on Micromachine Technologies and Systems*, pages 24–31, Tokyo, Japan, Oct. 1993.

[13] H. Hitakawa. Advanced parts orientation system has wide application. *Assembly Automation*, 8(3), 1988.

[14] J. D. Jacobson, S. H. Goodwin-Johansson, S. M. Bobbio, C. A. Bartlet, and N. Yadon. Integrated force arrays: Theory and modeling of static operation. *Journal of Microelectromechanical Systems*, 4(3):139–150, Sept. 1995.

[15] O. Khatib. Real time obstacle avoidance for manipulators and mobile robots. *Int. Journal of Robotics Research*, 5(1):90–99, Spring 1986.

[16] W. Liu and P. Will. Parts manipulation on an intelligent motion surface. In *IROS*, Pittsburgh, PA, 1995.

[17] T. McGeer. Passive dynamic walking. *Int. Journal of Robotics Research*, 1990.

[18] R. E. Mihailovich, Z. L. Zhang, K. A. Shaw, and N. C. MacDonald. Single-crystal silicon torsional resonators. In *Proc. IEEE Workshop on Micro Electro Mechanical Systems (MEMS)*, pages 155–160, Fort Lauderdale, FL, Feb. 1993.

[19] P. Moncevicz, M. Jakiela, and K. Ulrich. Orientation and insertion of randomly presented parts using vibratory agitation. In *ASME 3rd Conference on Flexible Assembly Systems*, September 1991.

[20] M. H. Raibert, J. K. Hodgins, R. R. Playter, and R. P. Ringrose. Animation of legged maneuvers: jumps, somersaults, and gait transitions. *Journal of the Robotics Society of Japan*, 11(3):333–341, 1993.

[21] J. Reif and H. Wang. Social potential fields: A distributed behavioral control for autonoomous robots. In K. Goldberg, D. Halperin, J.-C. Latombe, and R. Wilson, editors, *Algorithmic Foundations of Robotics*, pages 431–459. K. Peters, Wellesley, MA, 1995.

[22] E. Rimon and D. Koditschek. Exact robot navigation using artificial potential functions. *IEEE Transactions on Robotics and Automation*, 8(5), October 1992.

[23] K. A. Shaw, Z. L. Zhang, and N. C. MacDonald. SCREAM I: A single mask, single-crystal silicon process for microelectromechanical structures. In *Transducers — Digest Int. Conf. on Solid-State Sensors and Actuators*, Pacifico, Yokohama, Japan, June 1993.

[24] Z. L. Zhang and N. C. MacDonald. An RIE process for submicron, silicon electromechanical structures. *Journal of Micromechanics and Microengineering*, 2(1):31–38, Mar. 1992.